NASA Technical Memorandum 83631

Select Fiber Composites for Space Applications: A Mechanistic Assessment

C. A. Ginty and C. C. Chamis
Lewis Research Center
Cleveland, Ohio

Prepared for the
Twenty-ninth SAMPE Symposium and Exhibition
Reno, Nevada, April 3-5, 1984

NASA

TABLE OF CONTENTS

SELECT FIBER COMPOSITES FOR SPACE APPLICATIONS: A MECHANISTIC ASSESSMENT

C. A. Ginty* and C. C. Chamis**

National Aeronautics and Space Administration
Lewis Research Center
Cleveland, Ohio 44135

SUMMARY

Three fiber composites (graphite-fiber epoxy, graphite-fiber aluminum, and graphite-fiber magnesium) are evaluated for their possible use in space applications. Using the composite mechanics theories for thermomechanical behavior embodied in the ICAN (Integrated Composites Analyzer) computer code, select composite thermal and mechanical properties are predicted and also their response to cryogenic temperatures, resembling those which occur in space applications. The predicted results are presented in graphical form as a function of the composite's laminate configuration, fiber volume ratio and the selected use temperature. These results are suitable for preliminary design purposes only and should serve as an aid in selecting controlled experiments for obtaining corresponding measured data.

INTRODUCTION

The use of fiber composites in space applications is increasing. With this increase, reliable methods for predicting a material's properties in the space environment are required. Particular attention must be paid to the thermo-cyclic behavior of fiber composites when subjected to temperatures ranging from cryogenic or deep space to relatively high temperatures due to solar heating.

In this investigation, composite mechanics theories developed at Lewis Research Center for hygrothermomechanical behavior and embodied in the ICAN (Integrated Composites Analyzer) computer code were used to predict select composite thermal and mechanical properties and how they are affected by varying use cryogenic temperatures.

Three fiber composites: graphite-fiber/epoxy, graphite-fiber/aluminum, and graphite-fiber/magnesium were selected for evaluation. The thermal properties include heat capacity, heat conductivity, and the coefficient of thermal expansion. The mechanical properties include elastic and shear moduli, Poisson's ratio, and the lamination residual stress. These properties are presented graphically as a function of the laminate configuration and fiber volume ratio. In this form, they provide useful and convenient information for preliminary design purposes only since the theoretical predictions have not been verified with measured data as yet.

---

*Aerospace Structures Engineer.
**Aerospace Structures/Composites Engineer.

Finally, the credibility of the composite mechanics theories employed, the data obtained, and their significance as a reliable means of predicting composite behavior in space applications, will be discussed. Suggestions are also made on controlled test methods to experimentally determine these, and other properties, required in the thermo-mechanical design of composite space structures.

COMPOSITE MECHANICS THEORIES

Composite mechanics theories developed at Lewis Research Center for hygro-thermomechanical behavior consist of composite micromechanics, composite mechanics, and laminate theory. These theories require constituent material (fiber/matrix) properties in order to predict the composite ply properties (including geometric, mechanical, thermal and hygral (ref. 1)) as well as laminate properties. These theories are incorporated into a computer program, ICAN, also developed at Lewis. ICAN (Integrated Composites ANalyzer) was used in this investigation to predict the thermal and mechanical properties of selected composites. The input to ICAN consists of the constituent material properties (at ambient room temperature) as shown in table I, fiber volume ratio (FVR), void volume ratio, laminate geometric configuration, and data on the fabrication process. Output includes geometric, thermal, mechanical, and hygral properties of the composite at the ply and laminate levels.

Using ICAN the thermal properties (heat capacity, heat conductivity, and the coefficient of thermal expansion), the mechanical properties (elastic and shear moduli and Poisson's ratio) and residual stress are predicted as a function of: fiber volume ratio, composite system (the fiber properties (E_{11}, E_{22}, G_{12}, G_{23} and ν_{12}) and the matrix properties (E and ν)), laminate configuration (unidirectional ([0]), cross-plied ($[0/90]_S$) and quasi-isotropic ($[0/\pm60]_S$)) and cryogenic temperatures.

THEORETICAL RESULTS

Using the computer code ICAN, three composite systems are evaluated to determine their thermal and mechanical properties when subjected to different temperatures. The systems chosen are graphite-fiber/epoxy (G/E), graphite-fiber/aluminum (G/Al), and graphite-fiber/magnesium (G/Mg). The investigation includes [0], $[0/90]_S$, and $[0/\pm60]_S$ laminates. In addition, each laminate is evaluated as a function of increasing fiber volume ratio (FVR) including 0.5, 0.6, and 0.7.

The evaluation of the G/E laminate is conducted under three thermal conditions: 70° F, -320° F, and -423° F which corresponds to room temperature, liquid oxygen temperature, and liquid hydrogen temperature respectively. The latter two being typical temperatures encountered in space propulsion structures.

The metal matrix composites (G/Al and G/Mg) analyses are based on two thermal conditions: 70° F, and -200° F corresponding to room temperature and the temperature anticipated in space communication structures.

Predicted Thermal Properties

For each laminate the thermal properties, heat capacity (C), heat conductivity (K), and the coefficient of thermal expansion (α), are summarized graphically for convenient use. These properties were selected because of their significance in designing space structures for specified thermal distortion design requirements (ref. 2). The graphical results are plotted as a function of the fiber volume ratio (FVR) range and temperatures mentioned previously.

Heat capacity - (C). - Figure 1 shows C for the unidirectional G/E laminate while figure 2 displays C for the $[0/90]_S$ and $[0/\pm60]_S$ laminates. Note that the latter two laminates exhibit the same values for C. For the G/E laminates, the most substantial change in C occurs for the room temperature conditions; with an increase in FVR, C decreases. For the liquid oxygen and hydrogen temperature conditions C is hardly affected by the FVR.

The set of three laminates constructed of G/Al all result in the same values of C (figs. 3 and 4). Once again it is observed that C decreases much more rapidly at room temperature than at -200° F.

The heat capacity of G/Mg laminates is also independent of laminate configuration; therefore, the value of C for the unidirectional, $[0/90]_S$ and $[0/\pm60]_S$ laminates is the same (figs. 5 and 6). For the G/Mg laminates C undergoes a decrease for both thermal conditions as FVR increases. This decrease is more predominate for room temperature conditions.

Heat conductivity - (K). - Predicted results for this thermal property are summarized in terms of direction; either longitudinal or transverse to the composite structural axis and through the thickness as is indicated on the schematic accompanying each graph.

For the G/E unidirectional laminate (fig. 7) all values of K increase with increasing FVR. When comparing these values with their associated use temperatures, as the use temperature decreases, K decreases. For the $[0/90]_S$ and $[0/\pm60]_S$ laminates; K also increases with increasing FVR and has the same magnitude for all use temperatures (fig. 8).

For the G/Al unidirectional laminate in figure 9, it is observed that as a function of increasing FVR, K in the longitudinal direction increases while in the transverse direction it decreases slightly. For the $[0/90]_S$ and $[0/\pm60]_S$ laminates, K which is independent of direction increases with increasing FVR (fig. 10).

Figure 11 shows the G/Mg unidirectional laminate where K exhibits a significant increase in the longitudinal direction and a slight increase in the transverse direction. For the $[0/90]_S$ and $[0/\pm60]_S$ laminates (fig. 12), K increases with increasing FVR.

Coefficient of thermal expansion - (α). - For all G/E laminates, α decreases with increasing FVR (figs. 13 and 14). For the unidirectional laminate, α in the longitudinal direction is the same for all use temperatures. For the $[0/90]_S$ and $[0/\pm60]_S$ laminates, α is independent of direction; however, it is observed that with decreasing use temperatures, α decreases.

Figures 15 and 16 display α for the G/Al laminates. As expected since this is a matrix dominated property, α decreases with increasing FVR. For the unidirectional laminate, the magnitude of α in the transverse direction is much higher than that in the longitudinal.

The results for the unidirectional (fig. 17) and angle-ply (fig. 18) G/Mg laminates, indicate that α is exhibiting the same characteristics observed for the G/Al laminates above.

Predicted Mechanical Properties

The results of the mechanical properties are summarized as follows: moduli, both elastic (E) and shear (G) and Poisson's ratio (υ). Each of these is depicted as a function of both FVR and use temperature. These mechanical properties were selected because of their significance in the design of space structures to meet specified mechanical design requirements such as deflections, structural instabilities, and vibration frequencies (ref. 2).

Elastic and shear moduli - (E) and (G). - For the unidirectional G/E laminate (fig. 19) all values for the elastic and shear moduli increase with increasing FVR and also increase with a decrease in use temperature. For the angle-ply laminates, $[0/90]_S$ (fig. 20) and $[0/\pm60]_S$ (fig. 21), the moduli increase with increasing FVR. The elastic moduli are independent of direction and their magnitude is lowest in the $[0/\pm60]_S$ laminates.

Figure 22 shows the unidirectional G/Al laminate where E in the longitudinal direction increased while all other properties decreased. For the $[0/90]_S$ laminate (fig. 23) E and G are independent of direction; E increases while G decreases for increasing FVR. For the $[0/\pm60]_S$ laminate (fig. 24), G_{cyz} is the only property which decreases slightly with increasing FVR. All properties increase with decreasing use temperature; E for the $[0/90]_S$ laminate (fig. 23) exhibits the greatest increase while G_{cyz} for the $[0/\pm60]_S$ laminate (fig. 24) exhibits the smallest (almost negligible) decrease.

The unidirectional G/Mg laminate exhibits a substantial increase in longitudinal E when compared to the decrease the other properties undergo (fig. 25). The $[0/90]_S$ laminate (fig. 26) follows a similar trend. Figure 27 depicts an increase in E and G_{cxy} and a small decrease in G_{cyz} for the $[0/\pm60]_S$ laminate. These properties increase only slightly with decreasing use temperature.

Poisson's ratio - (υ). - For the unidirectional G/E laminate the values of υ are independent of use temperature and decrease with increasing FVR (fig. 28). For the $[0/90]_S$ laminate (fig. 29), υ also decreases with increasing FVR. In this case, the magnitude of υ_{cyz} is much greater than υ_{cxy}. Figure 30 displays υ for the $[0/\pm60]_S$ laminate which behaves in a similar manner as the $[0/90]_S$ laminate. There is, however, very little difference in magnitude between υ_{cxy} and υ_{cyz}. The values for υ decrease somewhat with decreasing use temperature for both laminates.

For the G/Al unidirectional laminate (fig. 31), υ is independent of use temperature and decreases as FVR increases. The $[0/90]_S$ laminate in figure 32 shows υ decreasing also with increasing FVR; however, the change is more dramatic for υ_{cxy}. For the $[0/\pm60]_S$ laminate (fig. 33), υ_{cxy}

increases while ν_{cyz} decreases. The values of ν experience very little change with decreasing use temperature.

The Poisson's ratio of G/Mg laminates (figs. 34 to 36) is behaving in a similar fashion as a function of FVR and use temperature as was observed for the G/Al laminates.

Lamination Residual Stresses

The residual stress as referred to here is the result of the change in the typical fabrication temperature of the laminate and the temperature at which the laminate is assumed to be used (use temperature) (ref. 3). These lamination residual stresses may induce transply cracks when their magnitudes reach values comparable to uniaxial ply strengths.

For the G/E laminate, the cure temperature is 370° F. Figure 37 displays σ_r for this laminate at use temperatures of 70° F, -320° F, and -423° F. A slight decrease is observed as the FVR increases. In the longitudinal direction σ_r is in compression while in the transverse direction it is in tension. As the difference between fabrication temperature and use temperature increases, σ_r increases. The lamination transverse residual stresses are about 60 percent of the estimated corresponding ply strengths at these use temperatures indicating no transply cracking.

For the G/Al (fig. 38) and G/Mg (fig. 39) laminates the fabrication temperature of 900° F was used to predict the σ_r at 70° F, -200° F, and -10° F. Viewing the results, it appears that for these laminates, FVR has very little effect on σ_r. The magnitude of the lamination residual transverse stresses is about 20 percent of the estimated corresponding ply strengths for G/Al laminate and about 30 percent of the G/Mg laminate indicating that no matrix yielding occurs in either laminate.

DISCUSSION

Using the computer code ICAN, with its multi-level composite micromechanics capability, analyses can be conducted on a variety of fiber composite systems and laminate configurations to computationally determine their suitability in space applications. The input for the analyses are constituent material candidates, composite systems, and laminate configuration, FVR, and the selected use temperatures typically resembling those encountered in space applications. The output results in a vast amount of data relating the composite's thermal and mechanical properties to the varying corresponding use temperatures. These data are best summarized in graphical form and can be used as an aid in selecting composites and laminate configurations during the preliminary design phase of space structural components. Though the results summarized are only for simple system composites "thoroughbreds", ICAN has the computational capability to effectively handle interply hybrids, intraply hybrids, superhybrids and combinations as well.

While ICAN can be used to predict a vast amount of data for thermal and mechanical properties, this data needs to be correlated with that measured from controlled experiments. The controlled experiments should include, as a

minimum, measurement of constituent material properties, ply properties, cross-plied ($[0/90]_S$), and quasi-isotropic ($[0/\pm60]_S$) properties in at least two different cryogenic environments. The predicted results summarized herein can serve as guides in selecting composite systems, laminate configurations, fiber volume ratios and test temperatures. Precision and accuracy of test data are very important in view of the fact that thermal distortions need to be kept to tolerances of a few percent of microstrain (ref. 4). The results summarized herein are not by any means complete for the entire thermomechanical design of composite structures in space environments. Additional thermomechanical properties associated with (1) heat transfer due to radiation; and (2) structural integrity degradation/enhancement in space environments also need to be determined experimentally. Concomitantly corresponding composite mechanics theories need to be developed to describe these additional thermomechanical properties.

No direct comparisons of predicted results presented with available measured data are made on an absolute value basis because of (1) the scarsity of measured data; and (2) incomplete information of whatever little measured data are available. Qualitatively, however, the predicted results appear to be consistent with limited data on thermal conductivity (ref. 5), on thermal expansion coefficients (refs. 5 to 7) and on moduli (refs. 5 and 8) for resin-matrix composites. More importantly, and on a relative basis, the influence of FVR, temperature and laminate configuration on the predicted thermal and mechanical properties summarized herein should be in very close, if not exact, agreement with measured data.

SUMMARY OF RESULTS

The salient results of an investigation on the theoretical prediction of select thermal and mechanical properties of fiber composite structures for space applications are as follows:

(1) The Lewis developed computer code ICAN (Integrated Composites Analyzer) is an effective means to computationally predict a variety of composite properties in space environments.

(2) The influence of composite system, laminate configuration, cryogenic temperature and fiber volume ratio (FVR) are readily evaluated.

(3) Predicted results show that composite system (graphite-fiber/epoxy (G/E), graphite-fiber/aluminum (G/Al), and graphite-fiber/magnesium (G/Mg)) have significant influence on the laminate thermomechanical properties as expected.

(4) Laminate configuration (unidirectional ([0]), cross-plied ($[0/90]_S$) and quasi-isotropic ($[0/\pm60]_S$)) also has significant influence on the laminate thermomechanical properties.

(5) Cryogenic temperatures affect the thermal and mechanical (moduli (normal and shear)) properties of G/E unidirectional composites, but has insignificant influence on those of the G/E $[0/90]_S$ and $[0/\pm60]_S$ laminates. Cryogenic temperatures have no effect on the Poisson's ratio of G/E [0] composites and a slight effect on those for the $[0/90]_S$ and $[0/\pm60]_S$ laminates.

(6) Cryogenic temperatures have negligible effect on the thermal and mechanical properties of G/Al and G/Mg [0], $[0/90]_S$, and $[0/\pm 60]_S$ laminates.

(7) Fiber volume ratio has significant effects on the thermomechanical properties of G/E composites, particularly those at room temperature and those which are fiber dominated, but relatively insignificant effects on those of G/Al and G/Mg composites.

(8) The lamination residual stresses will not induce transply cracking in the G/E laminate. Likewise, the G/Al and G/Mg laminates will not experience matrix yielding.

(9) The predicted thermomechanical properties summarized herein are appropriate for use only in preliminary designs since they have not been correlated with measured data.

(10) Controlled experiments are needed to obtain measured data of constituent materials, [0], $[0/90]_S$ and $[0/\pm 60]_S$ candidate composites for space applications. These data can then be used to verify existing composite mechanics theories and can be used as a basis to develop new ones.

REFERENCES

1. Chamis, C. C., "Simplified Composite Micromechanics Equations for Hygral, Thermal and Mechanical Properties," NASA TM-83320, 1983.

2. Adsit, N. R., "Composites for Space Applications," ASTM Stand. News, 11, pp. 20-23, 1983.

3. Chamis, C. C., "Residual Stress in Angleplied Laminates and their Effects on Laminate Behavior," NASA TM-78835, 1978.

4. Advanced Composites - Special Topics, Technology Conferences, El Segundo, California, 1979, pp. 313-402.

5. Askins, D. R., "Development of Engineering Data on Advanced Composite Materials," AFWAL-TR-81-4172, WPAFB, Ohio, February 1982.

6. Short, J. S., Hyer, M. W., and Bowles, D. E., "Development of a Priest Interferometer for Measurement of the Thermal Expansion of Graphite-Epoxy in the Temperature Range 116-366 K," NASA TM-85176, 1982.

7. Cairns, D. S., Adams, D. F., "Moisture and Thermal Expansion of Composite Materials," (UWME-DR-101-104-1) Composite Materials Research Group, Wyoming Univ., Laramie, November 1981.

8. Klich, P. J., and Cockrell, C. E., "Mechanical Properties of a Fiberglass Prepreg System at Cryogenic and Other Temperatures," AIAA J., 21, 1722-1728, 1983.

TABLE I. - FIBER AND MATRIX PROPERTIES

Property			Material			
Name	Symbol	Units	Fiber	Matrix		
			Graphite	Epoxy	Aluminum	Magnesium
Number of fibers/end	N_f	----	10,000	-------	------	------
Diameter of fiber	d_f	in.	0.0003	-------	------	------
Density	ρ	lb/in^3	0.0630	0.0443	0.0950	0.0600
Longitudinal modulus	E_{11}	mpsi	31.0	0.5	10.0	6.0
Transverse modulus	E_{22}	mpsi	2.0	-------	------	------
Shear modulus	G_{12}	mpsi	2.0	[a]0.1852	[a]3.759	[a]2.308
Shear modulus	G_{23}	mpsi	1.0	-------	------	------
Longitudinal Poisson's ratio	ν_{12}	in./in.	0.200	0.350	0.330	0.300
Transverse Poisson's ratio	ν_{23}	in./in.	0.250	-------	------	------
Longitudinal coefficient of thermal expansion	α_{11}	10^{-6}in./in./°F	-0.550	42.8	12.9	14.0
Transverse coefficient of thermal expansion	α_{22}	10^{-6}in./in./°F	5.60	-------	------	------
Longitudinal heat conductivity	K_{11}	Btu/hr/ft^2/°F/in.	580.0	1.25	104.0	44.0
Transverse heat conductivity	K_{22}	Btu/hr/ft^2/°F/in.	58.0	-------	------	------
Heat capacity	C	Btu/lb/°F	0.170	0.250	0.230	0.240
Tensile strength	S_T	ksi	400	15	52	40
Compressive strength	S_C	ksi	400	35	52	40
Shear strength	S_S	ksi	0	13	26	25
Void conductivity	K_v	Btu/hr/ft^2/°F/in.	------	0.225	0.225	0.225
Glass transition temperature/melting temperature[b]	T_{GD}/T_M	°F	------	420	1080	1050

[a]G_{12} for the matrix is calculated using the elastic modulus and Poisson's ratio.
[b]Melting temperature is associated with the metal matrix and glass transition temperature with the epoxy matrix.

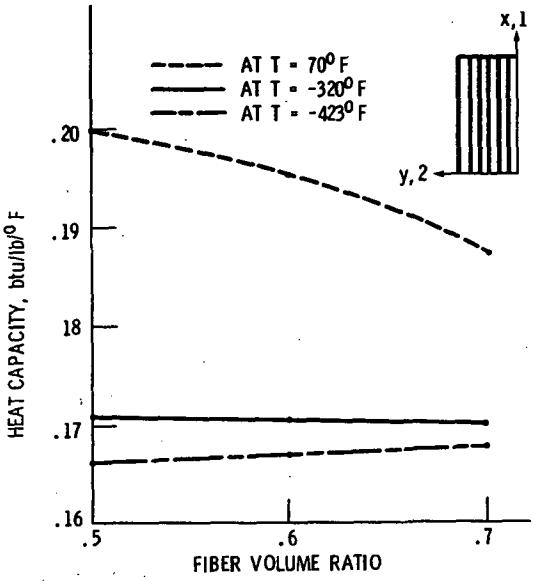

Figure 1. - Heat capacity for a graphite epoxy unidirectional laminate.

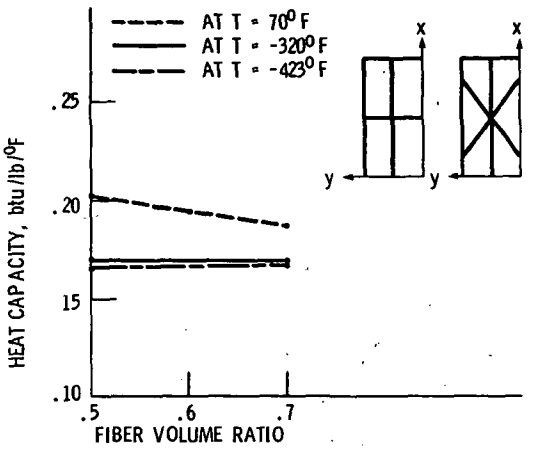

Figure 2. - Heat capacity for graphite epoxy $[0/90]_s$ and $[0/\pm 60]_s$ laminates.

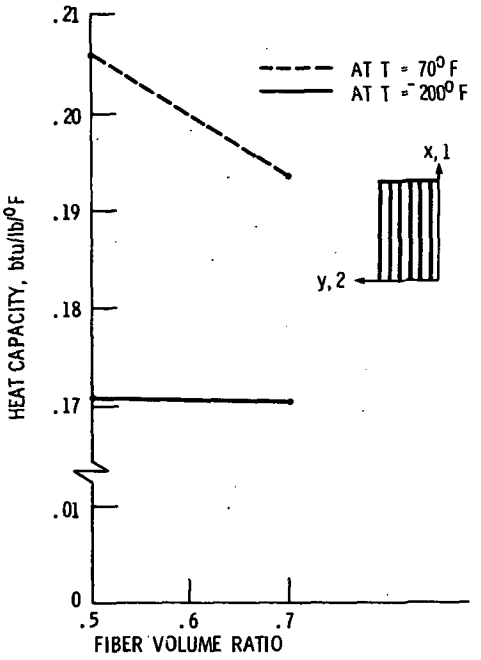

Figure 3. - Heat capacity for a graphite aluminum unidirectional laminate.

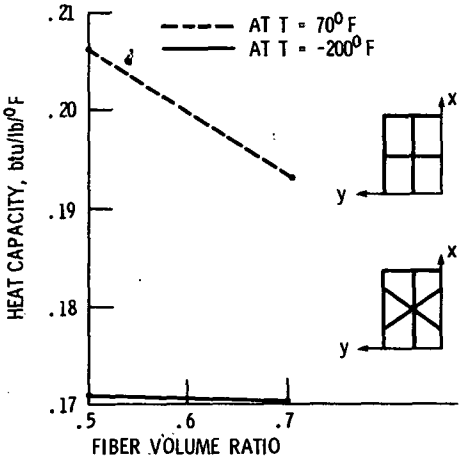

Figure 4. - Heat capacity for graphite aluminum $[0/90]_s$ and $[0/\pm 60]_s$ laminates.

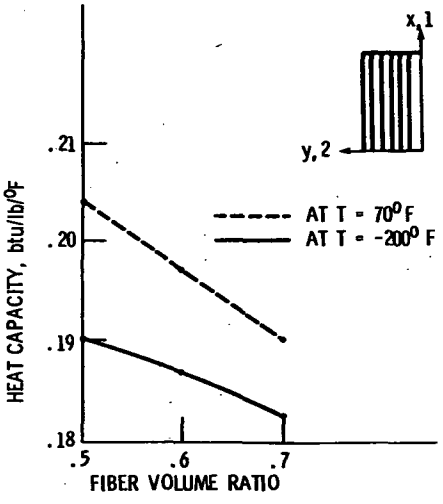

Figure 5. - Heat capacity for a graphite magnesium unidirectional laminate.

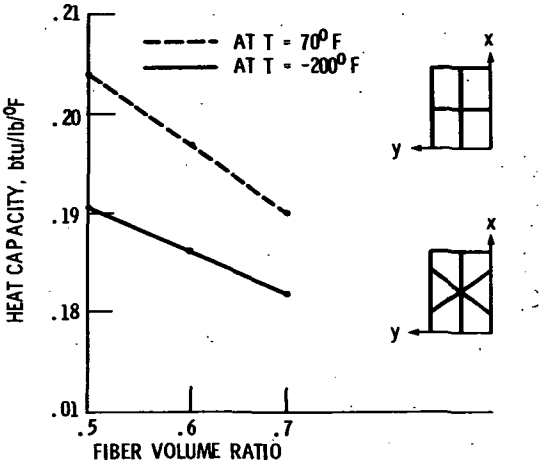

Figure 6. - Heat capacity for graphite magnesium $[0/90]_s$ and $[0/\pm 60]_s$ laminates.

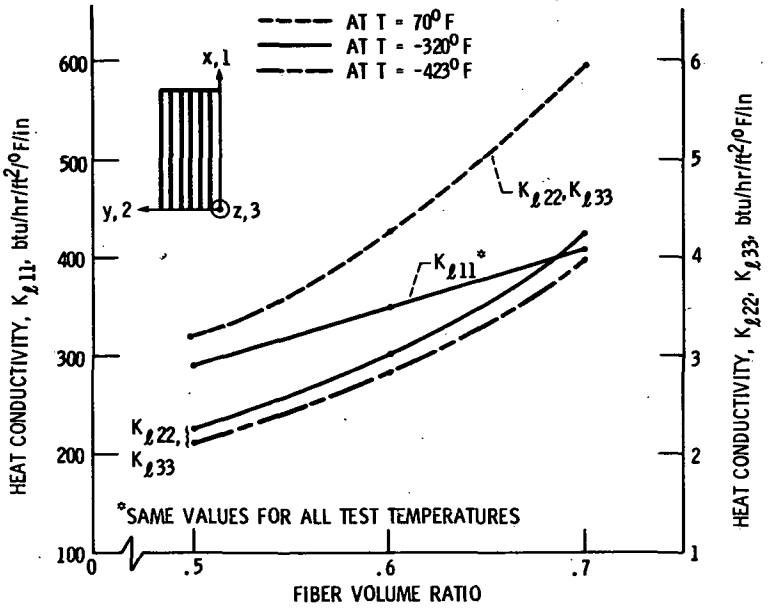

Figure 7. - Heat conductivity for a graphite epoxy unidirectional laminate.

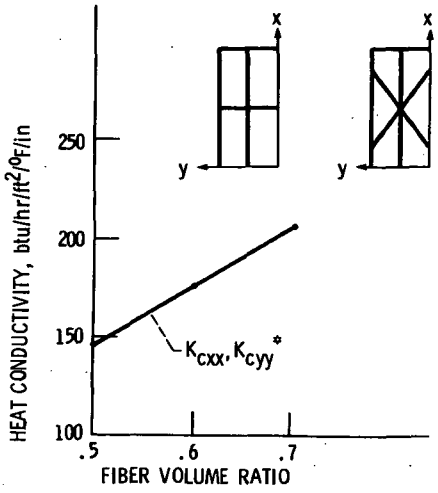

Figure 8. - Heat conductivity for graphite epoxy $[0/90]_S$ and $[0/\pm 60]_S$ laminates. *Same value for all temperatures.

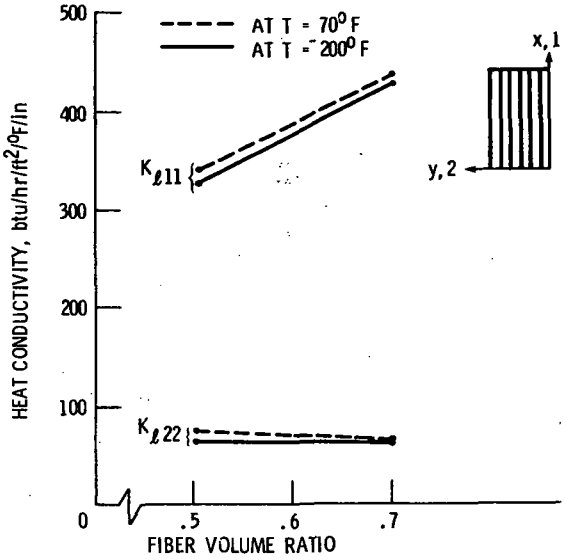

Figure 9. - Heat conductivity for a graphite aluminum unidirectional laminate.

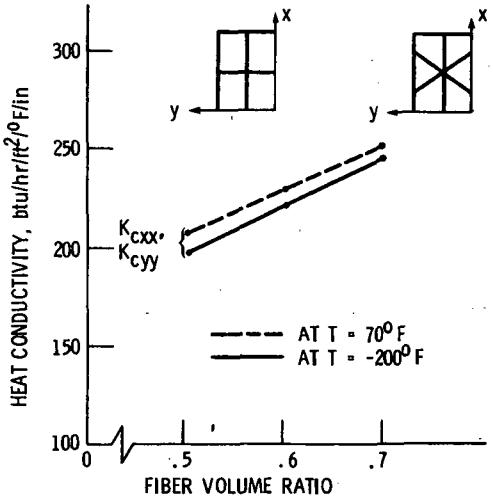

Figure 10. - Heat conductivity for graphite aluminum $[0/90]_S$ and $[0/\pm 60]_S$ laminates.

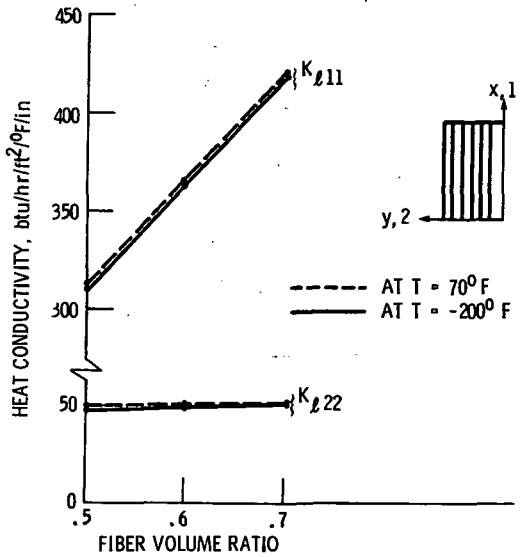

Figure 11. - Heat conductivity for a graphite magnesium unidirectional laminate.

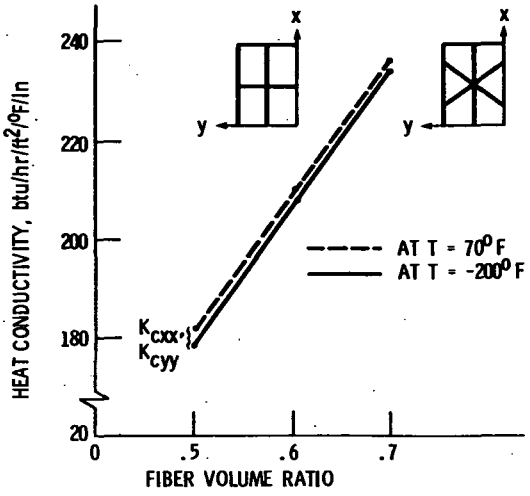

Figure 12. - Heat conductivity for graphite magnesium $[0/90]_s$ and $[0/\pm 60]_s$ laminates.

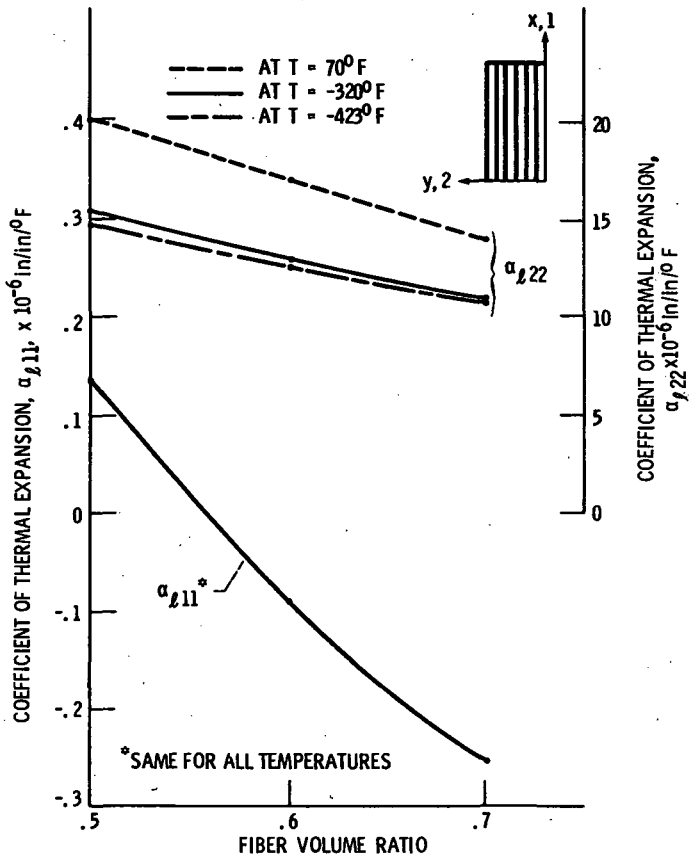

Figure 13. - Coefficient of thermal expansion for a graphite epoxy unidirectional laminate.

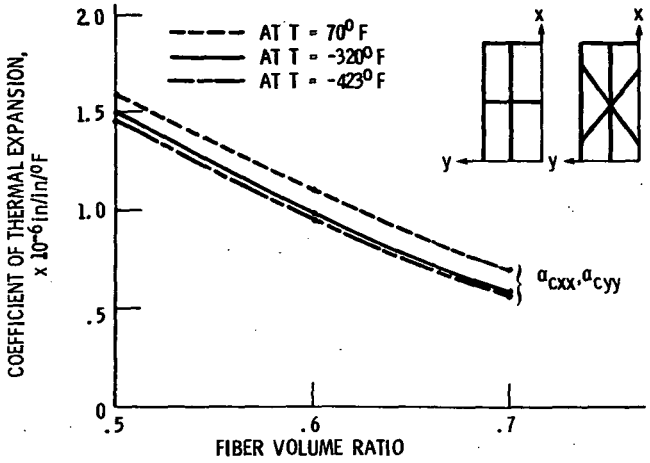

Figure 14. - Coefficient of thermal expansion for graphite epoxy $[0/90]_S$ and $[0/\pm 60]_S$ laminates.

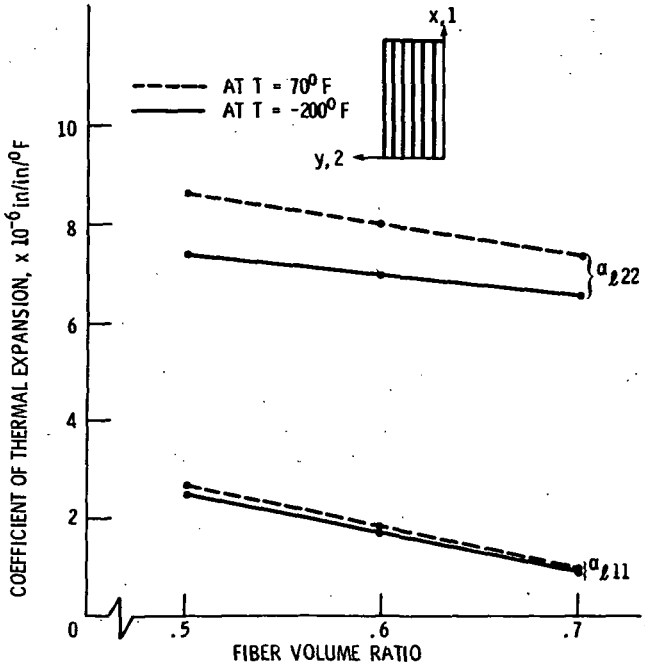

Figure 15. - Coefficient of thermal expansion for a graphite aluminum unidirectional laminate.

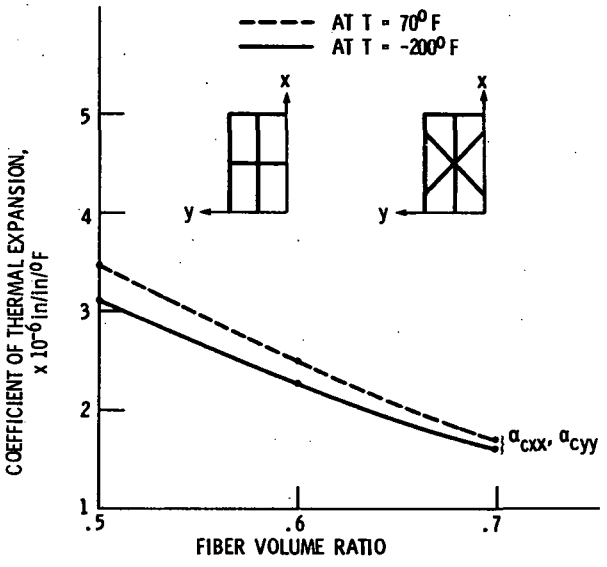

Figure 16. - Coefficient of thermal expansion for graphite aluminum $[0/90]_s$ and $[0/\pm 60]_s$ laminates.

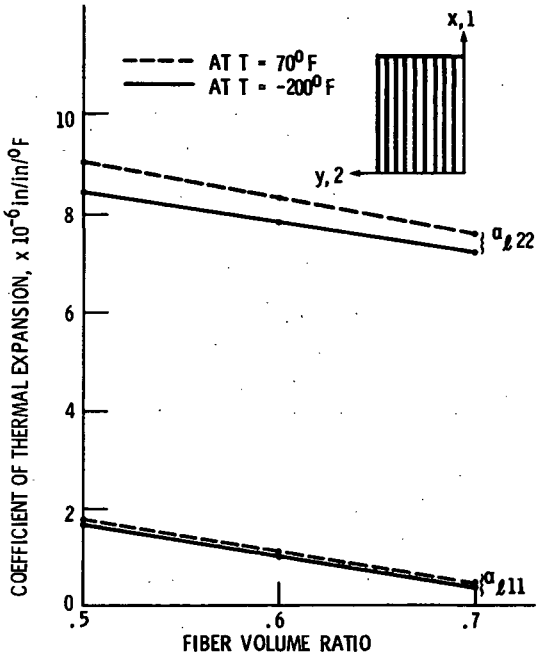

Figure 17. - Coefficient of thermal expansion for a graphite magnesium unidirectional laminate.

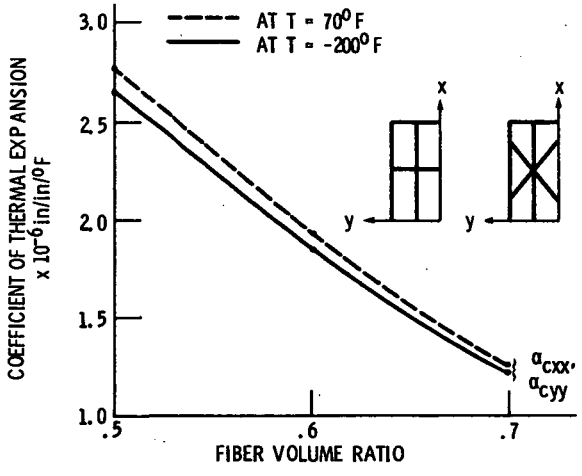

Figure 18. - Coefficient of thermal expansion for graphite magnesium $[0/90]_s$ and $[0/\pm 60]_s$ laminates.

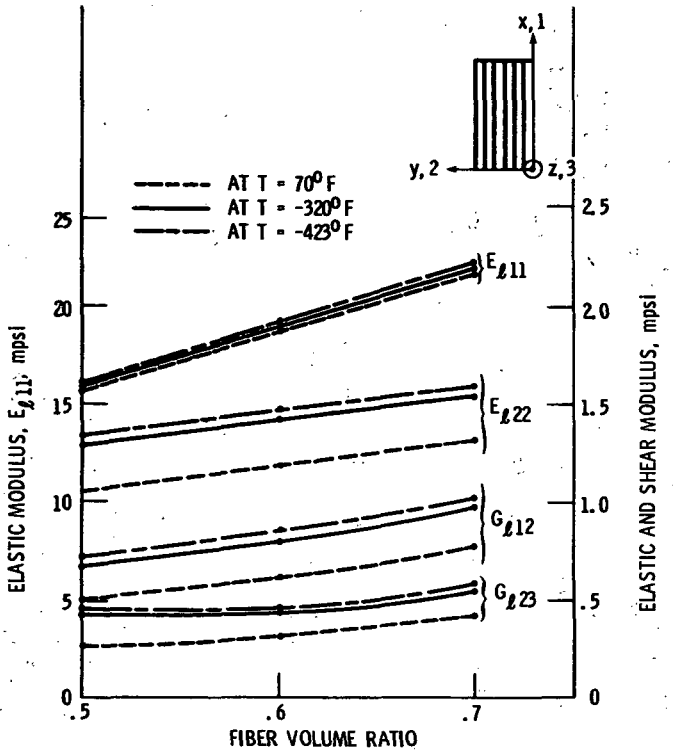

Figure 19. - Moduli for a graphite epoxy unidirectional laminate.

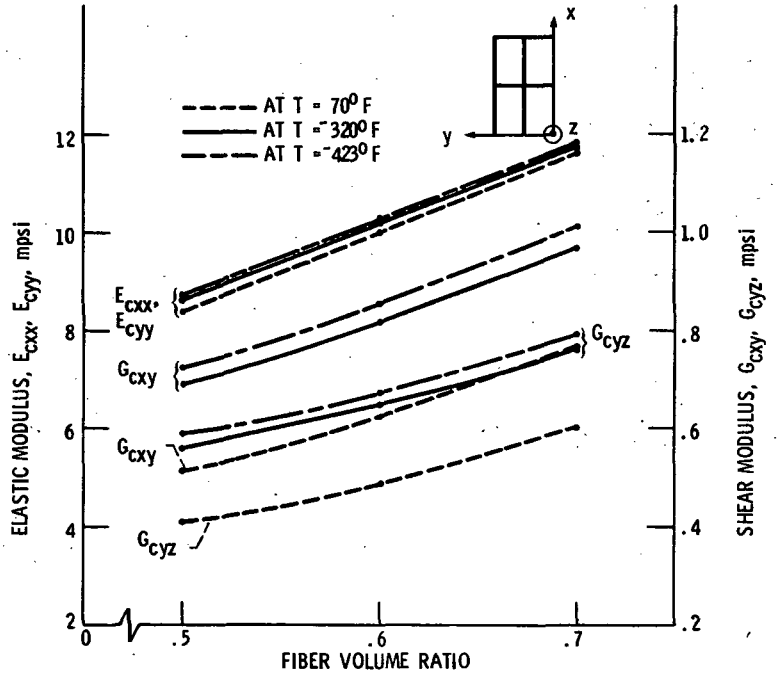

Figure 20. - Moduli for a graphite epoxy $[0/90]_s$ laminate.

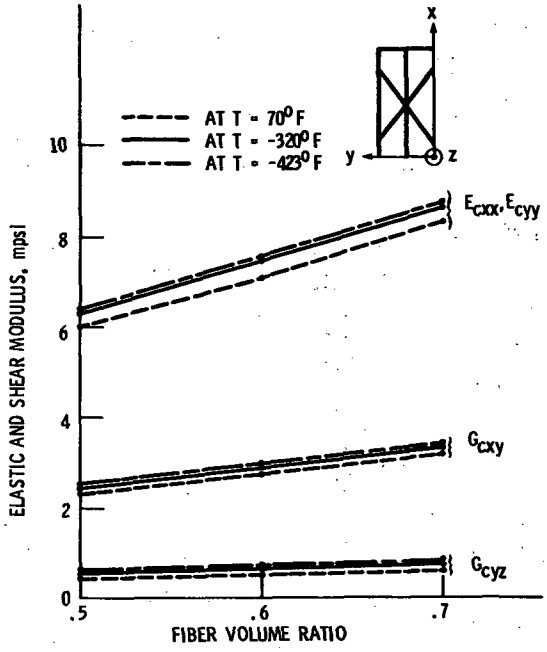

Figure 21. - Moduli for a graphite epoxy $[0/\pm 60]_S$ laminate.

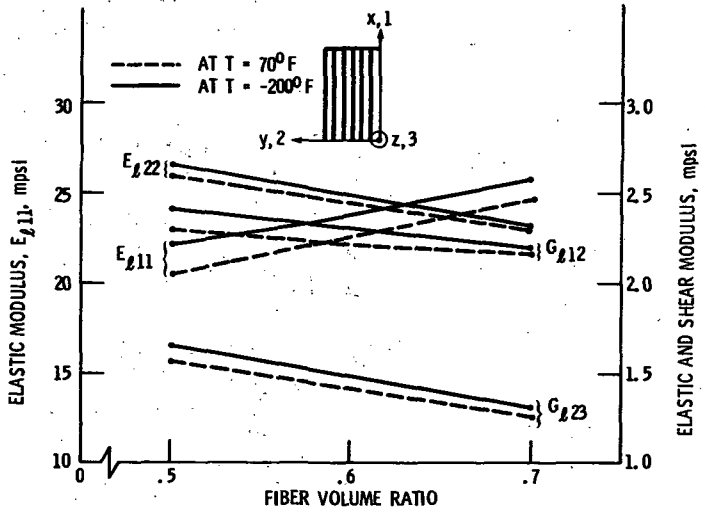

Figure 22. - Moduli for a graphite aluminum unidirectional laminate.

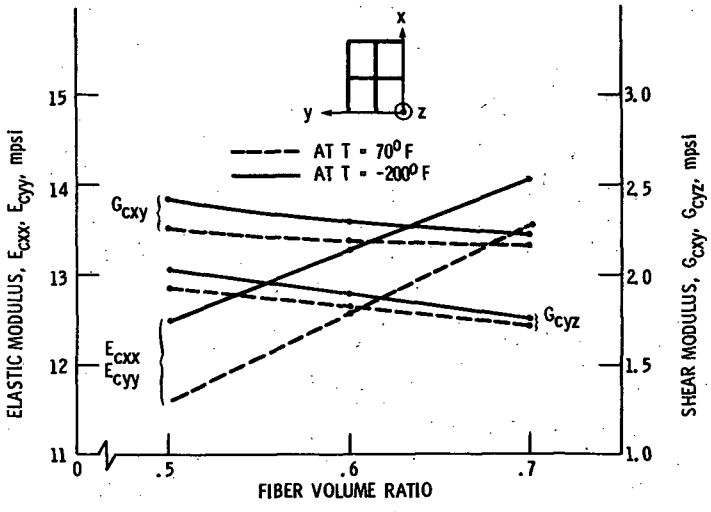

Figure 23. - Moduli for a graphite aluminum $[0/90]_S$ laminate.

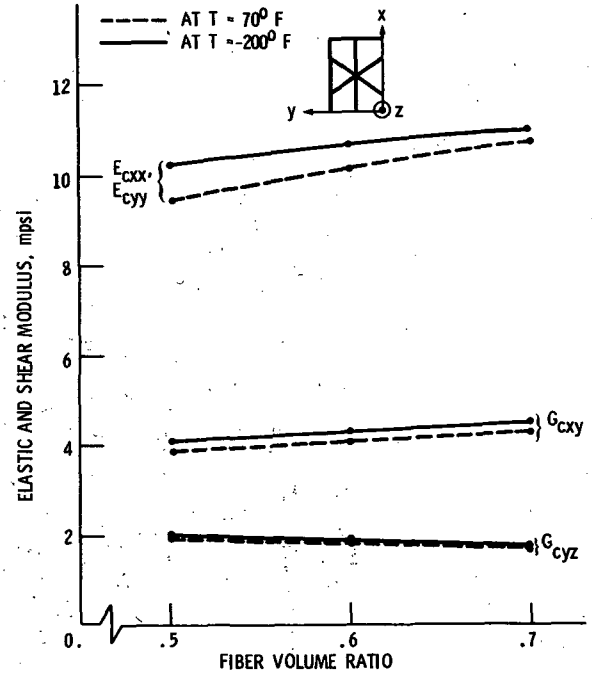

Figure 24. - Moduli for a graphite aluminum $[0/\pm 60]_S$ laminate.

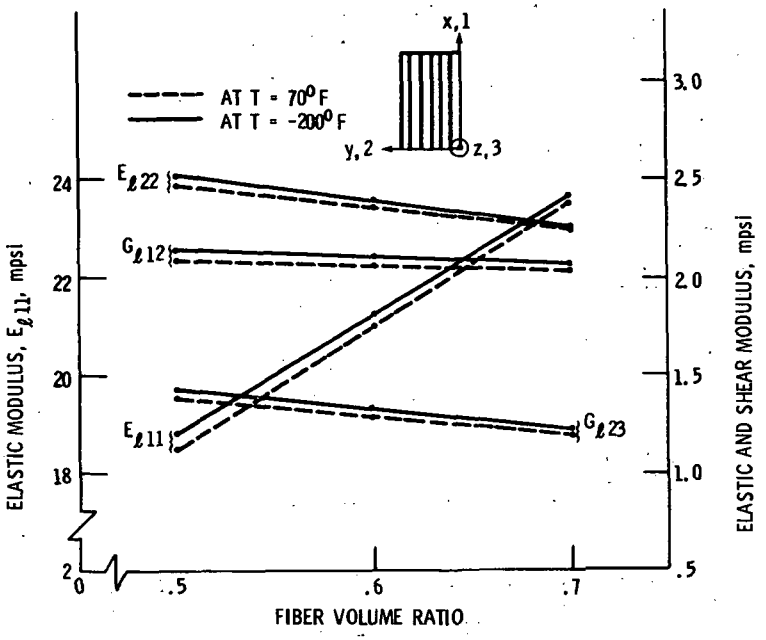

Figure 25. - Moduli for a graphite magnesium unidirectional laminate.

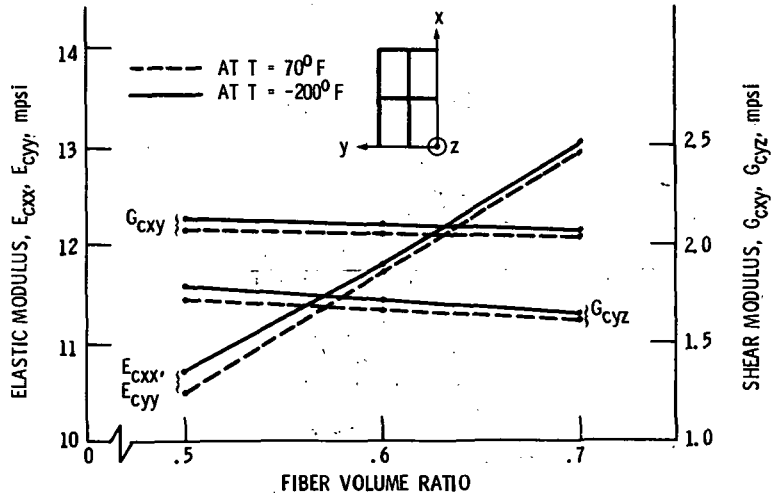

Figure 26. - Moduli for a graphite magnesium $\left[0/90\right]_s$ laminate.

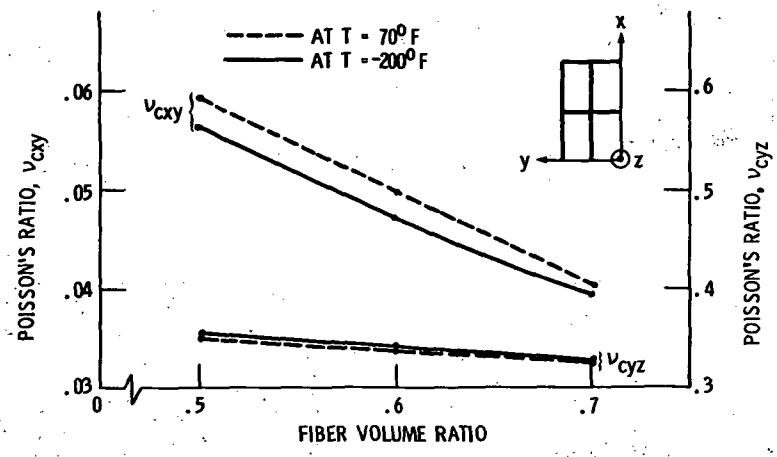

Figure 32. - Poisson's ratio for a graphite aluminum $[0/90]_s$ laminate.

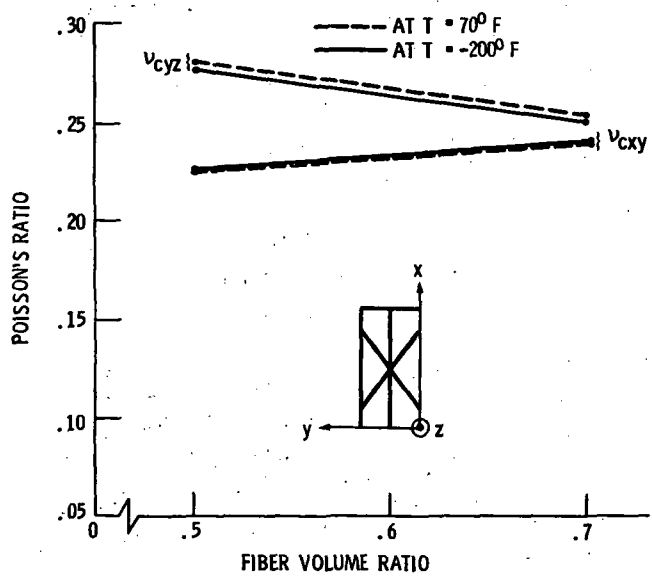

Figure 33. - Poisson's ratio for a graphite aluminum $[0/+60]_s$ laminate.

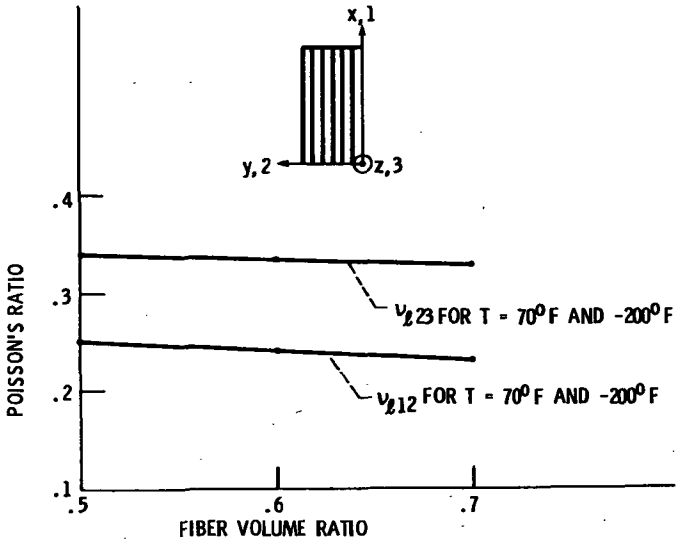

Figure 34. - Poisson's ratio for a graphite magnesium unidirectional laminate.

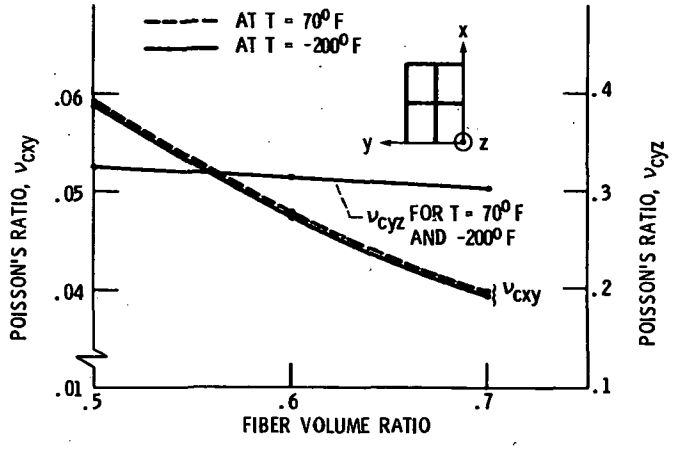

Figure 35. - Poisson's ratio for a graphite magnesium $[0/90]_s$ laminate.

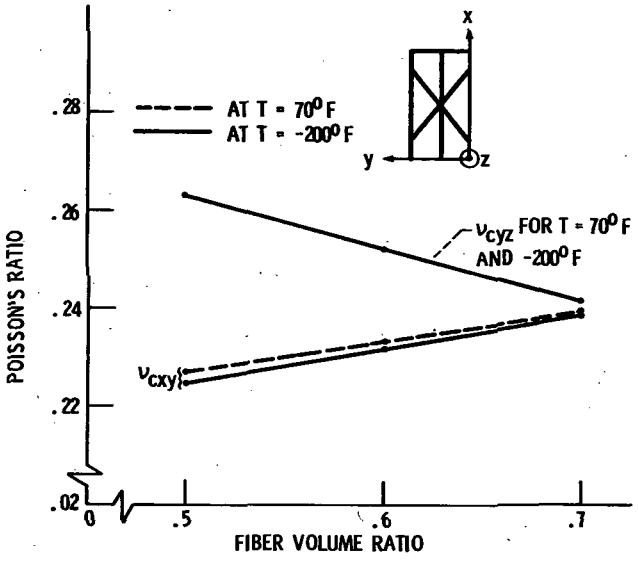

Figure 36. - Poisson's ratio for a graphite magnesium $[0/\pm 60]_s$ laminate.

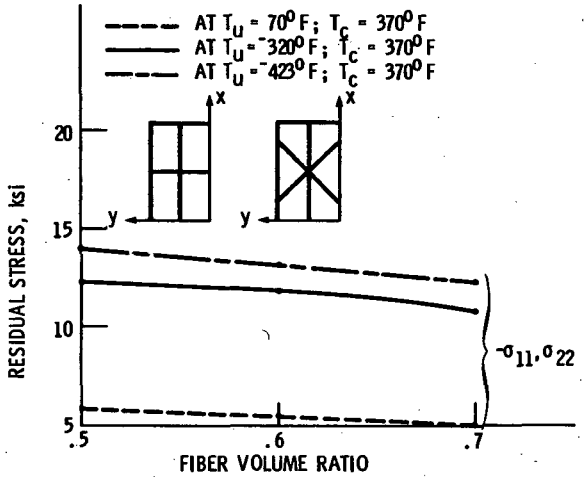

Figure 37. - Residual stress for graphite epoxy $[0/90]_s$ and $[0/\pm 60]_s$ laminates.

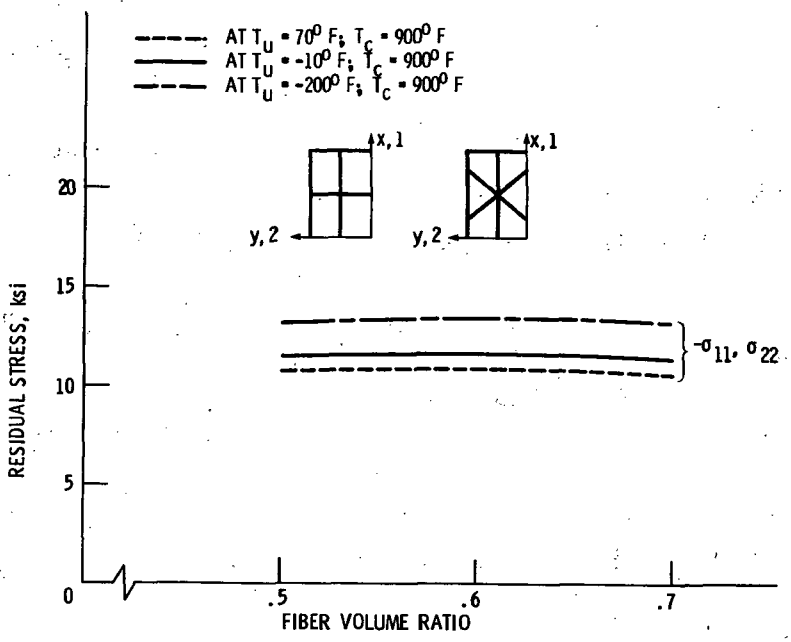

Figure 38. - Residual stress for graphite aluminum $[0/90]_s$ and $[0/\pm 60]_s$ laminates.

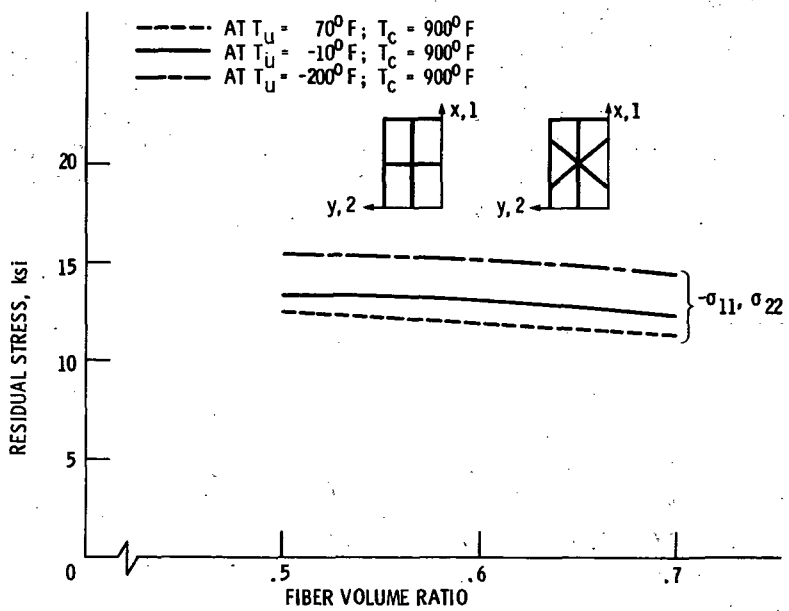

Figure 39. - Residual stress for graphite magnesium $[0/90]_s$ and $[0/\pm 60]_s$ laminates.

1. Report No.	2. Government Accession No.	3. Recipient's Catalog No.
NASA TM-83631		

4. Title and Subtitle	5. Report Date
Select Fiber Composites for Space Applications: A Mechanistic Assessment	6. Performing Organization Code 505-33-5B

7. Author(s)	8. Performing Organization Report No.
C. A. Ginty and C. C. Chamis	E-2069
	10. Work Unit No.

9. Performing Organization Name and Address	11. Contract or Grant No.
National Aeronautics and Space Administration Lewis Research Center Cleveland, Ohio 44135	13. Type of Report and Period Covered Technical Memorandum

12. Sponsoring Agency Name and Address	14. Sponsoring Agency Code
National Aeronautics and Space Administration Washington, D.C. 20546	

15. Supplementary Notes

Prepared for the Twenty-ninth SAMPE Symposium and Exhibition, Reno, Nevada, April 3-5, 1984.

16. Abstract

Three fiber composites (graphite-fiber epoxy, graphite-fiber aluminum, and graphite-fiber magnesium) are evaluated for their possible use in space applications. Using the composite mechanics theories for thermomechanical behavior embodied in the ICAN (Integrated Composites Analyzer) computer code, select composite thermal and mechanical properties are predicted and also their response to cryogenic temperatures, resembling those which occur in space applications. The predicted results are presented in graphical form as a function of the composite's laminate configuration, fiber volume ratio and the selected use temperature. These results are suitable for preliminary design purposes only and should serve as an aid in selecting controlled experiments for obtaining corresponding measured data.

17. Key Words (Suggested by Author(s))	18. Distribution Statement
Fiber composites; Space applications; Thermomechanical theories; Thermal properties; Mechanical properties; Fiber volume ratio; Unidirectional laminates; Cross-plied laminates; Quasi-isotropic laminates; Graphite fibers; Epoxy matrix; Aluminum matrix; Magnesium matrix	Unclassified - unlimited STAR Category 24

19. Security Classif. (of this report)	20. Security Classif. (of this page)	21. No. of pages	22. Price*
Unclassified	Unclassified		

*For sale by the National Technical Information Service, Springfield, Virginia 22161

National Aeronautics and
Space Administration

Washington, D.C.
20546

Official Business
Penalty for Private Use, $300

SPECIAL FOURTH CLASS MAIL
BOOK

Postage and Fees Paid
National Aeronautics and
Space Administration
NASA-451

NASA

POSTMASTER: If Undeliverable (Section 158
Postal Manual) Do Not Return